0026-895X/96/030547-09$3.00/0

MOLECULAR PHARMACOLOGY, 49:547–555 (1996).

N-[5-Nitro-2-furfurylidene]-3-amino-2-oxazolidinone Activation by the Human Intestinal Cell Line Caco-2 Monitored through Noninvasive Electron Spin Resonance Spectroscopy

LUISA ROSSI, ISABELLA DE ANGELIS, JENS Z. PEDERSEN, ELIANA MARCHESE, ANNALAURA STAMMATI, GIUSEPPE ROTILIO, and FLAVIA ZUCCO

Department of Biology, University of Rome "Tor Vergata," Rome, Italy (L.R., E.M., G.R.), Comparative Toxicology and Ecotoxicology Laboratory, Istituto Superiore di Sanità, Rome, Italy (I.D., A.S.), CNR Institute for Experimental Medicine, Rome, Italy (J.Z.P.), and CNR Institute of Biomedical Technologies, Rome, Italy (F.Z.)

Received June 7, 1995; Accepted November 8, 1995

SUMMARY

The pathways participating in the metabolism of the nitrofuran antimicrobial drug *N*-[5-nitro-2-furfurylidene]-3-amino-2-oxazolidinone (furazolidone) in intact cells were investigated in the human intestinal cell line Caco-2. One-electron reduction of furazolidone led to the formation of a free radical intermediate that could be monitored in dense cell suspensions by noninvasive electron spin resonance spectroscopy. The effects of enzyme inhibitors on the kinetics of radical production and decay were used to estimate the relative contribution of different enzymes to the reductive activation of the drug. Although many enzymes are known to reduce nitrofurans *in vitro* (e.g., xanthine oxidase, aldehyde oxidase, DT-diaphorase, mitochondrial redox chain components), their contributions were insignificant in living Caco-2 cells. The first reducing equivalent required for the formation of the nitroanion derivative of furazolidone appeared to be provided essentially by the microsomal cytochrome P450 reductase. This was confirmed through studies of the NADPH-dependent radical formation by microsomes. Differentiated Caco-2 cells, an established enterocyte model, showed only modestly increased radical formation and the same enzyme-specificity pattern as undifferentiated cells. Consistently, only a small increase in P450 reductase activity was found in differentiated cells, in contrast to the 10-fold increase seen for typical differentiation marker enzymes. With the electron spin resonance method that we describe, it is possible to distinguish between sites of bioactivation of redox active drugs in intact cells.

Many nitroheterocyclic compounds are known antimicrobial agents and potential radiosensitizers (1, 2), but their therapeutic use is severely limited by toxic effects, including mutagenicity and carcinogenicity (3–5). The toxicity of these compounds has been explained on the basis of their intracellular reduction to reactive intermediates. The first step of the activation may produce a nitroanion free radical species that is rapidly reoxidized by molecular oxygen to the parent compound, with the concomitant formation of the superoxide anion. This process is known as redox cycling and generates a continuous flux of superoxide, leading to the formation of other reactive oxygen intermediates such as hydrogen peroxide and hydroxyl radicals, which are strong oxidants that are able to impair cellular functions (6–8). Furthermore, oxygen consumption during redox cycling may result in hypoxic conditions, which allow further reduction of the nitroanion radical to nitroso derivatives and a variety of other reactive intermediates and stable end-products (1, 9, 10). Some of these intermediates are strongly electrophilic and bind covalently to proteins and nucleic acids (1, 11–13). Cell injury caused in this way is now considered to be the principal reason for the antimicrobial effect, but damage produced by redox cycling may be important for the general cytotoxicity of nitroheterocyclic drugs.

Many possible routes of activation of these xenobiotics have been outlined, mainly through initial reduction by flavoproteins, such as xanthine oxidase, aldehyde oxidase, and cytochrome P450[1] reductase; by components of the mitochondrial redox chain; or by DT-diaphorase (1, 7–10, 14). However, most studies have been carried out with purified enzymes or subcellular fractions, and therefore the main pathway responsible for activation *in vivo* has not been singled out. There are few techniques available for the study of metabolism in intact cells.

This work was supported in part by the CNR Special Projects FATMA and ACRO and by the European Union Research Project AIR 2-CT93–0860.

[1] Cytochrome P450 nomenclature in this work follows the convention of Nebert *et al.* (44).

ABBREVIATIONS: ESR, electron spin resonance; DPI, diphenylene iodonium; ID, iodonium diphenyl; furazolidone, *N*-[5-nitro-2-furfurylidene]-3-amino-2-oxazolidinone; SKF-525A, *N,N*-diethylaminoethyl-2,2-diphenylvalerate.

The 5-nitrofuran drug furazolidone is commonly used against gastrointestinal infections in humans and as a prophylactic feed additive in animal husbandry. However, it is known to cause cardiomyopathy in poultry (15) and possibly also in humans, where several side effects have been described (16, 17). Residues of both the parent compound and its toxic metabolites in edible tissues of treated animals may therefore represent a health hazard for the human consumer.

The gastrointestinal tract represents the first barrier against ingested drugs and thus is a likely target for furazolidone. A good model for this tissue is represented by the Caco-2 cell line, a human colorectal carcinoma cell line that has been used to study various functions of intestinal cells (18–21). Despite its origin, this cell line differentiates spontaneously into cells that show morphological, functional, and enzymatic characteristics of small intestine enterocytes, including microvilli and polarized distribution of brush border enzymes (18, 22). The use of this intestinal cell line for toxicological studies is validated by the discovery that both undifferentiated and differentiated Caco-2 cells possess phase I and phase II biotransforming activities (23–26). In a recent study, we showed that Caco-2 cells are susceptible to furazolidone to a degree related to their state of differentiation; fully differentiated cells are less sensitive, with an LD_{50} of 550 μM compared with the value of 380 μM found for undifferentiated cells (27). The activities of antioxidant enzymes such as superoxide dismutase, glutathione reductase, glutathione peroxidase, and catalase may increase on differentiation (28, 29); for the latter two enzymes, even 5–10-fold higher levels can be reached (28). However, it is not yet known whether the lower sensitivity of differentiated cells is a consequence of the induction of defense enzymes or is caused by changes in the pathways of furazolidone metabolism.

In the present report, we used a noninvasive analytical technique, ESR spectroscopy, to monitor the formation of the furazolidone nitroanion radical by intact Caco-2 cells. This approach, rarely applied in studies of whole-cell metabolism, allowed us to follow the intracellular activation of the drug without perturbation of cellular integrity. The contribution of potential nitrofuran reducing enzymes to furazolidone activation has been determined through the effect of inhibitors on the kinetics of radical formation and decay. Our results point to the microsomal P450 reductase as the prevailing site of furazolidone reduction in both undifferentiated and differentiated Caco-2 cells.

Materials and Methods

Chemicals. Allopurinol, 3-amino-1,2,4-triazole, antimycin A, cyanamide, dicoumarol, disulfiram, furazolidone, metyrapone, and rotenone were purchased from Sigma Chemical Co. (St. Louis, MO); chloral hydrate and potassium cyanide were purchased from Fluka (Buchs, Switzerland); and ID was purchased from Aldrich (Milwaukee, WI). SKF-525A was obtained from Research Biochemicals International (Natick, MA), and DPI was obtained from Alexis (Läufelfingen, Switzerland). Ficoll 400 was from Pharmacia (Sollentuna, Sweden). Furazolidone stock solutions were prepared in dimethylsulfoxide and protected from light.

Cell cultures. Caco-2 cells were cultured at 37° under 5% CO_2 atmosphere, essentially according to Pinto *et al.* (18). The cells were seeded in 75-cm^2 Falcon flasks (Becton-Dickinson, NJ) and grown in monolayers in Dulbecco's modified Eagle's medium (GIBCO, Paisley, UK) supplemented with 10% inactivated fetal calf serum, 4 mM glutamine, 1% (w/v) nonessential amino acids, 3.7 g/l sodium bicarbonate, 100 μg/ml streptomycin, and 100 IU/ml penicillin. After 7 days (undifferentiated cells) or 21 days (differentiated cells) of culture, the cells were detached by trypsin/EDTA treatment (0.2% trypsin, 2 mM EDTA), washed twice in Chance buffer (6.2 mM KCl, 145 mM NaCl, 11 mM sodium phosphate, pH 7.4), and counted. Cells used for the determination of enzyme activities were detached mechanically and washed twice in 140 mM NaCl, and 20 mM sodium phosphate, pH 7.4. The final cell pellet was resuspended in the same buffer. Cell viability was routinely estimated with the Trypan blue exclusion test.

Microsomal preparation. Rat liver microsomes were prepared by a sucrose gradient method according to Dallner (30). The final pellet was resuspended in 120 mM NaCl and 20 mM sodium phosphate buffer, pH 7.4, at a concentration of 30 mg protein/ml and stored under liquid nitrogen. Microsomes from undifferentiated Caco-2 cells were prepared according to Boulenc *et al.* (26). Briefly, the monolayer of a confluent culture in a 175-cm^2 flask was washed twice in 136 mM NaCl, 2.6 mM KCl, and 10 mM sodium phosphate, pH 7.4; mechanically detached; sonicated; and homogenized. The suspension was centrifuged at 9000 × *g* for 20 min, and the supernatant was recentrifuged at 105,000 × *g* for 1 hr. Finally, the pellet was resuspended in a small volume of phosphate buffer with 1 mM EDTA and 20% glycerol. The microsomes were stored at −80° until use.

ESR measurements. Aliquots of 10–15 μl pelleted cells (1–4 × 10^6 cells/sample) were mixed with 25 μl Chance buffer containing 20% (w/v) Ficoll 400. The presence of Ficoll prevented sedimentation during the measurements and did not influence radical formation. Furazolidone and inhibitors were added from stock solutions in dimethylsulfoxide or water; a maximum of 4% dimethylsulfoxide was added to the samples. The final volume was adjusted to 50 μl by the addition of Chance buffer. Control experiments were made with the same addition of solvents. After the addition of furazolidone, the sample was immediately drawn into capillary tubes and measured at room temperature with a Bruker ESP300 spectrometer equipped with a high sensitivity TM_{110}-mode cavity. Spectra were normally recorded with 20 mV microwave power, 1 G modulation, and a scan time of 42 sec; high resolution spectra were obtained with samples in flat glass capillaries, 5 mW power, and a modulation of 100 mG. Normally, 20 scans were accumulated to improve the signal-to-noise ratio. For kinetics measurements, an overmodulation of 10 G was applied to broaden the spectrum and eliminate signal changes due to minor variations in the frequency. The time course of radical formation was determined by monitoring continuously the height of the highest line in the spectrum; kinetics were normally followed over a period of 20 min.

Spectrophotometric measurements. Optical spectra were recorded with a Perkin Elmer Lambda-9 instrument. Measurements of the metabolism of furazolidone in suspensions of Caco-2 cells were made using flat glass capillaries of 0.30-mm light path (Camlab, Cambridge, UK) placed inside a 1-mm-wide cuvette in the cell holder of the spectrophotometer. Samples of 4 × 10^6 cells in Chance buffer containing 10% Ficoll were prepared exactly as for the ESR measurements, except that the final volume was 100 μl. Spectra were taken at 3-min intervals. The extinction coefficient of furazolidone at 367 nm was measured to be 19.6 mM^{-1} cm^{-1}.

Oxygen uptake measurements. Oxygen consumption was measured at 25° with a Clark-type oxygen electrode (Gilson Oxygraph 5/6 H). Cells from a single flask of confluent differentiated or undifferentiated cells were detached with trypsin, washed, and counted, and aliquots were diluted in Chance buffer to reach a final cell concentration of 2.7 × 10^6 cells/ml in the oxygraph chamber (final volume, 1.8 ml). After recording basal respiration for 5 min, we added mitochondrial electron transport inhibitors (1 mM KCN, 0.1 mM rotenone, or 0.1 mM antimycin A), followed by the addition of furazolidone at a final concentration of 0.5 mM. Oxygen uptake was expressed as nmol oxygen consumed/10^6 cells/min.

Catalase inactivation. Differentiated cells were treated with 27 mM aminotriazole for 6 hr at 37° in the growth medium. The cells were then washed twice with 136 mM NaCl, 2.6 mM KCl, and 10 mM sodium phosphate, pH 7.4, and incubated under standard culture conditions in growth medium containing 220 or 440 μM furazolidone. Toxicity was determined after 24 and 48 hr with the Neutral Red uptake test (31). Activity measurements consistently showed 92–93% inhibition of catalase activity in treated cells.

Enzyme assays. Activities of the differentiation marker enzymes alkaline phosphatase, sucrase-isomaltase, and catalase were determined as previously described (28). Cytochrome *c* (P450) reductase was measured in samples of cell homogenates obtained by sonication (3 × 10 sec, 4°) of cell suspensions in 140 mM NaCl and 20 mM sodium phosphate, pH 7.4. The activity was determined spectrophotometrically after the addition of 1.2 mM KCN (32). Data were expressed as nmol cytochrome *c* reduced/min/10^6 cells.

Results

Furazolidone radical formation. The addition of furazolidone to dense suspensions of undifferentiated Caco-2 cells resulted in the formation of a radical species that could be detected by ESR spectroscopy (Fig. 1a). The radical produced by Caco-2 cells was identical to that formed by rat liver microsomes in the presence of furazolidone and NADPH (Fig. 1b); the same spectrum could be obtained with the xanthine/xanthine oxidase system (not shown). No radicals were detected in the absence of furazolidone, cells, or microsomes (Fig. 1e). The ESR spectrum produced by the microsomes was sufficiently intense to be measured under high resolution conditions to determine the characteristic coupling constants (Fig. 1c). Through computer simulation of the experimental spectra, the radical was identified as the one-electron reduced furazolidone nitroanion species (Fig. 1d).

The kinetics of furazolidone radical generation by Caco-2 cells were reflected in the characteristic time course of the ESR signal (Fig. 2). The appearance of the radical signal was preceded by a lag phase, representing the time required to consume oxygen present in the sample. Once all oxygen was consumed, as a result of both basal cell respiration and furazolidone redox cycling, the radical accumulated and the ESR signal appeared. A maximum level was reached in 1–3 min, followed by a slow decay; almost-complete disappearance was observed after ~1 hr. Both the amount of radical formed and the duration of the lag phase depended on cell concentration; an increased radical signal and a correspondingly reduced lag phase were found when cell density was changed from 1 to 4 × 10^6 cells/sample (Fig. 2, a–c). A similar behavior was seen with increasing furazolidone concentrations up to a saturating level of ~1 mM (Fig. 2, b, d, and e).

Reintroduction of air to the sample caused disappearance of the radical signal, which returned after another lag phase (Fig. 2f). However, after complete decay of the signal, the introduction of air did not result in renewed generation of the radical, indicating that the product formed could not be oxidized back to furazolidone. The decay was caused only to a small extent by cell death because cell viability was >90%

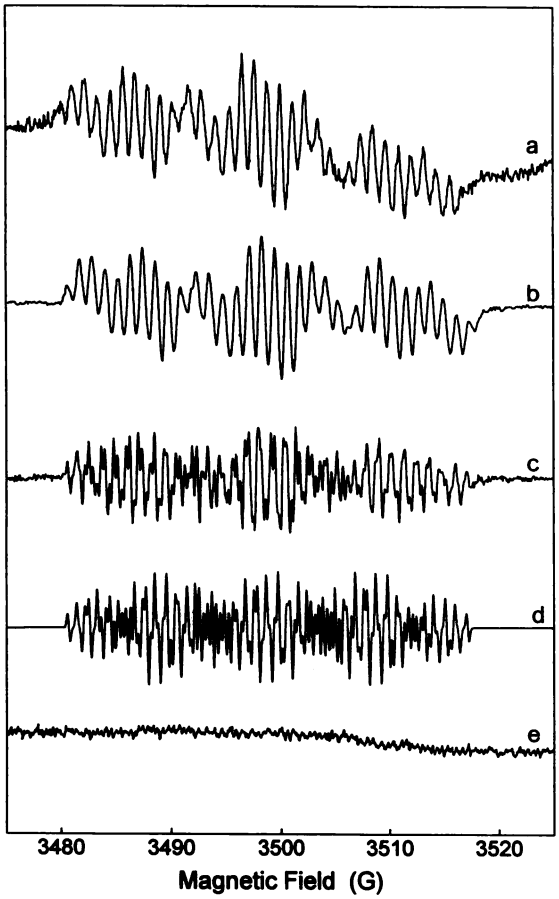

Fig. 1. ESR spectra of the furazolidone radical produced by Caco-2 cells or rat liver microsomes. Samples contained 1 mM furazolidone and 2 × 10^6 undifferentiated cells (a), 1.6 mg/ml microsomal protein plus 1 mM NADPH (b), or 1.6 mg/ml microsomal protein plus 5 mM NADPH (c). Spectrum (c) was recorded under high resolution conditions to allow comparison with the computer simulation (d), obtained with the following hyperfine constants: a_{N1} = 10.17 (NO_2^-), a_{N2} = 2.28 (N═CH), a_{N3} = 0.77 (>N—), a_{H1} = 5.27 (H4), a_{H2} = 2.00 (H3), a_{H3} = 0.88 (N═CH), a_{H4} = 1.03 (>N—CH_2), and a_{H5} = 1.11 (>N—CH_2). Spectrum (e) shows undifferentiated Caco-2 cells (2 × 10^6) in the absence of furazolidone.

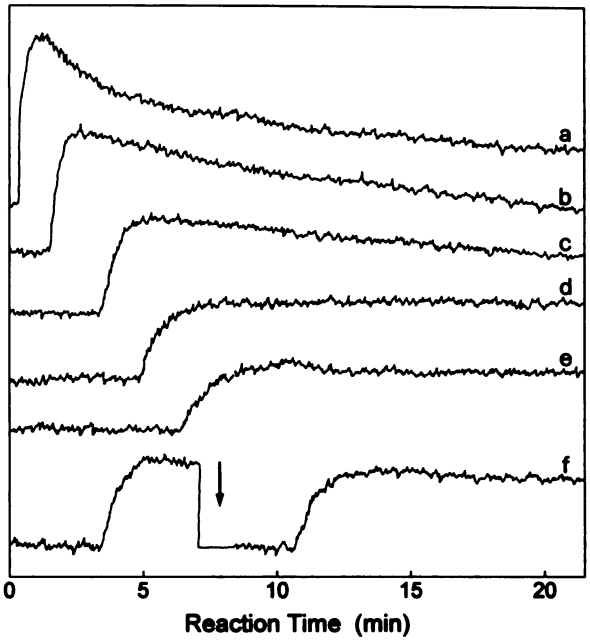

Fig. 2. Kinetics of furazolidone radical formation by undifferentiated Caco-2 cells. a, 4 × 10^6 cells, 1 mM furazolidone. b, 2 × 10^6 cells, 1 mM furazolidone. c, 1 × 10^6 cells, 1 mM furazolidone. d, 2 × 10^6 cells, 0.5 mM furazolidone. e, 2 × 10^6 cells, 0.1 mM furazolidone. f, 1 × 10^6 cells, 1 mM furazolidone. *Arrow*, point of introduction of air into the system.

throughout the experiments. The rate of decay was initially enhanced at high cell concentrations, suggesting that consumption of furazolidone resulted in a lower steady state level of the radical. Renewed addition of furazolidone at the end of a time course consistently regenerated the radical signal with similar intensity, although with slower kinetics compared with the initial signal (not shown). In contrast, the addition of 5 mM glucose to the samples did not have an effect on the kinetics, indicating that the decay of the radical signal was not due to exhaustion of intracellular reductants.

Effects of inhibitors. To investigate which reducing enzymes were primarily involved in the initial reduction of furazolidone by intact Caco-2 cells, we studied the effects of various enzyme inhibitors on the kinetics of the ESR signal (Table 1). The inhibition of an enzyme that generates the free radical would result in lower ESR signals and longer lag times, whereas inhibition of an enzyme that reduces the radical further to the nitroso derivative should give rise to higher radical signals and possibly also change the rate of signal decay. Inhibitors of the mitochondrial electron transport chain (rotenone, antimycin A, and KCN) caused a marked increase in the lag time before radical appearance (Fig. 3b). Once all oxygen was consumed, however, the radical signal reached the same level as in control samples, with the same rates of formation and decay. The longer lag phase was therefore not indicative of decreased radical production but rather was simply due to inhibition of endogenous oxygen consumption. Incubation with allopurinol, a specific inhibitor of xanthine oxidase, or with the aldehyde oxidase inhibitors disulfiram, cyanamide, and chloral hydrate did not alter the rate of appearance or the stability of the signal. The same result was found for dicoumarol, whether used at a low concentration (10 μM), where it acts as a DT-diaphorase inhibitor, or at higher doses (0.5 mM), where it has been shown to inhibit cytochrome b_5 reductase activity (33).

TABLE 1

Effect of enzyme inhibitors on the level of furazolidone radical formation in Caco-2 cells

Samples for ESR measurements were prepared and measured, as described in Materials and Methods. The radical level was determined as the height of the ESR signal relative to that of a control sample made with the same cell preparation and at the same time of incubation. The values shown were obtained by summing data from many different cell preparations; two to five experiments were made for each inhibitor concentration. Preincubation of inhibitors for 20 min at room temperature did not alter the results. Other than the effects of the iodonium compounds, the variations caused by the inhibitors were not statistically significant.

Treatment	Radical level
	%
Control	100 ± 11
KCN (2.5 mM)[a]	98 ± 7
Rotenone (4 μM)[b]	102 ± 10
Antimycin A (4 μM)[b]	95 ± 13
Carbon monoxide[c]	89 ± 20
SKF-525A (200 μM)[a]	97 ± 12
Metyrapone (400 μM)[a]	108 ± 5
ID (400 μM)	50 ± 8
ID (2 mM)	20 ± 3
DPI (400 μM)	10 ± 1
Disulfiram (200 μM)[a]	95 ± 2
Chloral hydrate (1 mM)[a]	99 ± 10
Cyanamide (500 μM)[a]	92 ± 4
Dicoumarol (8 μM)	101 ± 21
Dicoumarol (500 μM)	94 ± 9
Allopurinol (1 mM)[a]	109 ± 14

[a] Identical results were obtained with 10-fold lower concentrations.
[b] Identical results were obtained with 10-fold higher concentrations.
[c] Carbon monoxide-saturated samples.

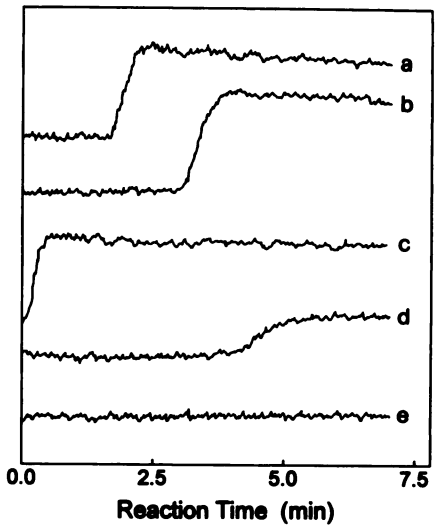

Fig. 3. Effect of various inhibitors of nitroreductases on the kinetics of furazolidone radical formation by undifferentiated Caco-2 cells. a, 2×10^6 cells plus 1 mM furazolidone. b, Same as a plus 4 μM rotenone, 4 μM antimycin or 2.5 mM KCN. c, Same as a saturated with carbon monoxide. d, Same as a plus 2 mM ID. e, Same as a plus 1 mM DPI.

The metabolism of most xenobiotics depends on microsomal cytochrome P450 activity, which is known to be present in Caco-2 cells (26, 34). However, inhibition of cytochrome P450 by either SKF-525A or metyrapone did not affect the kinetics of radical formation in the intact cells (Table 1). Also, carbon monoxide treatment did not alter the rate of radical formation or the amount of radical accumulated, except that in this case the lag phase was eliminated, since all oxygen was removed through flushing with carbon monoxide (Fig. 3c). Thus, cytochrome P450 apparently was not important during the two initial steps of furazolidone reduction that involve the free radical species. In contrast, the flavoprotein inhibitors ID and DPI had drastic effects on the kinetics. When furazolidone was added to samples of Caco-2 cells in the presence of either ID or DPI, the appearance of the radical was delayed and both the rate of formation and the final steady state level were lower than in the absence of inhibitors (Table 1 and Fig. 3). DPI proved to be much more potent than ID; despite the addition of 2 mM ID, a residual radical signal was still observed (Fig. 3d), whereas 1 mM DPI completely abolished the signal (Fig. 3e). Dose-dependence measurements were made to characterize the inhibitory effect of DPI; an IC_{50} of 60 μM was calculated (Fig. 4).

Activation by microsomes. The effects of ID and DPI indicated radical formation by cytochrome P450 reductase, which unfortunately cannot be inhibited specifically in intact cells. To examine this possibility, small quantities of microsomes were isolated from Caco-2 cells and incubated with 1 mM furazolidone and 1 mM NADPH. After consumption of the oxygen, the typical furazolidone radical ESR spectrum was observed; in contrast, no signal appeared when 1 mM DPI was included (results not shown). However, due to the limited amount of material that was obtainable, these microsomes were not suitable for kinetics measurements. Reduction of furazolidone by cytochrome P450 reductase was therefore studied with rat liver microsomes (Fig. 5). With the

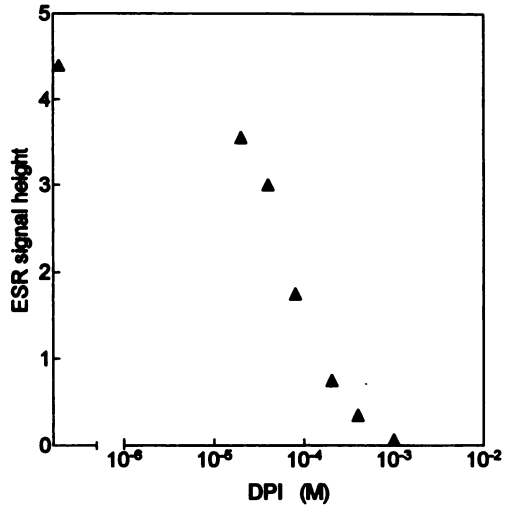

Fig. 4. Dose-dependence curve of DPI inhibition of furazolidone radical formation in undifferentiated Caco-2 cells. Data are shown for a single preparation of cells with samples of 50 μl containing 2×10^6 cells, 1 mM furazolidone, and varying amounts of DPI. The maximum height of the free radical ESR signal was measured in arbitrary units and plotted as a function of inhibitor concentration.

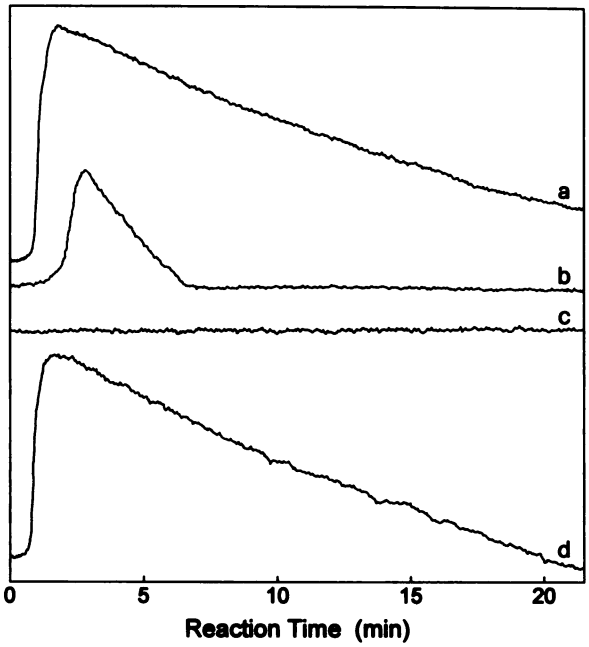

Fig. 5. Kinetics of furazolidone radical formation by rat liver microsomes. All samples contained 1.6 mg/ml microsomal protein in phosphate buffer, with the following additions: a, 1 mM furazolidone plus 1 mM NADPH; b, 0.5 mM furazolidone plus 0.5 mM NADPH; c, 1 mM furazolidone, 1 mM NADPH, plus 0.2 mM DPI; and d, 1 mM furazolidone, 1 mM NADPH, plus 1 mM SKF-525A.

use of furazolidone and NADPH concentrations in the millimolar range, radical formation was fast and the signal reached high levels. The signal did not remain at a plateau, however, but decayed slowly due to consumption of one of the substrates, as shown by the reappearance of the radical when more furazolidone or NADPH was added (not shown). These results indicated that the enzyme was not saturated even at high substrate concentrations. With lower NADPH and furazolidone concentrations, radical formation became progressively slower, the maximum level decreased, and decay of the signal was faster. In the presence of 0.2 mM DPI, generation of the radical was completely suppressed, whereas the addition of 1 mM SKF-525A or metyrapone did not affect the kinetics of signal formation and decay (Fig. 5).

Optical measurements of furazolidone reduction. The metabolism of furazolidone by Caco-2 cells could be monitored spectrophotometrically through the decrease in its characteristic absorption at 367 nm (Fig. 6). These experiments were carried out with the use of flat glass capillaries, which allowed measurements on dense cell suspensions under conditions identical to those for the samples studied with ESR; thus, the kinetics of furazolidone metabolism were the same for both spectroscopic approaches. In the presence of Caco-2 cells, an almost linear decrease of the height of the peak at 367 nm was observed; the rate of furazolidone reduction was 0.5 nmol/min/10^6 cells. The furazolidone spectrum disappeared almost completely within 2 hr without the formation of metabolites absorbing in the visible range. The reduction of furazolidone was strongly inhibited when DPI was introduced in the sample (Fig. 6b). Cell viability at the end of the measurements was higher than 90%, which is in agreement with the viability seen after ESR experiments.

Furazolidone metabolism in differentiated cells. Caco-2 cells cultured for 7 days are known to still be in the undifferentiated state. When the cells were cultured for 21 days, they differentiated and showed features resembling small intestine enterocytes (18). Differentiated cells generated furazolidone radicals more efficiently than undifferentiated cells (Fig. 7); the apparent differences in kinetics were due to the intrinsic higher metabolic activity of differentiated cells. Indeed, the time course of radical formation was very similar when samples of these cells were compared with samples containing approximately twice the number of undifferentiated cells. Also, the pattern of enzyme inhibition was similar for the two cell types: only the iodonium compounds were able to prevent radical formation, whereas none of the other inhibitors tested, including the specific cytochrome P450 inhibitors, affected the radical steady state level (data not shown).

The enhanced furazolidone metabolism capacity of differentiated Caco-2 cells was confirmed by oxygen uptake measurements. As shown in Table 2, furazolidone stimulated oxygen consumption by Caco-2 cells after mitochondrial respiration had been blocked by inhibitors. For cells in the differentiated state (21 days in culture), the rate of cyanide-resistant oxygen uptake was twice the rate found for undifferentiated cells, corresponding to a 2-fold higher free radical production capacity. For both cell types, consumption of oxygen due to furazolidone redox cycling was lower than the basal respiration rate (Table 2), which is in agreement with the previously reported observation that furazolidone increased oxygen uptake in the absence of respiratory chain inhibitors [79% and 87% for undifferentiated and differentiated Caco-2 cells, respectively (27)].

Differentiation of Caco-2 cells is accompanied by drastic changes in many enzyme activities that may increase to 5–100-fold the values of undifferentiated cells. The effect is particularly evident for enzymes characteristic of enterocytic development but is also seen for certain drug-metabolizing enzymes (23, 26). Given the probable role of cytochrome P450 reductase in furazolidone reduction, the activity of this enzyme in Caco-2 cells was examined. Only a 2-fold increase in

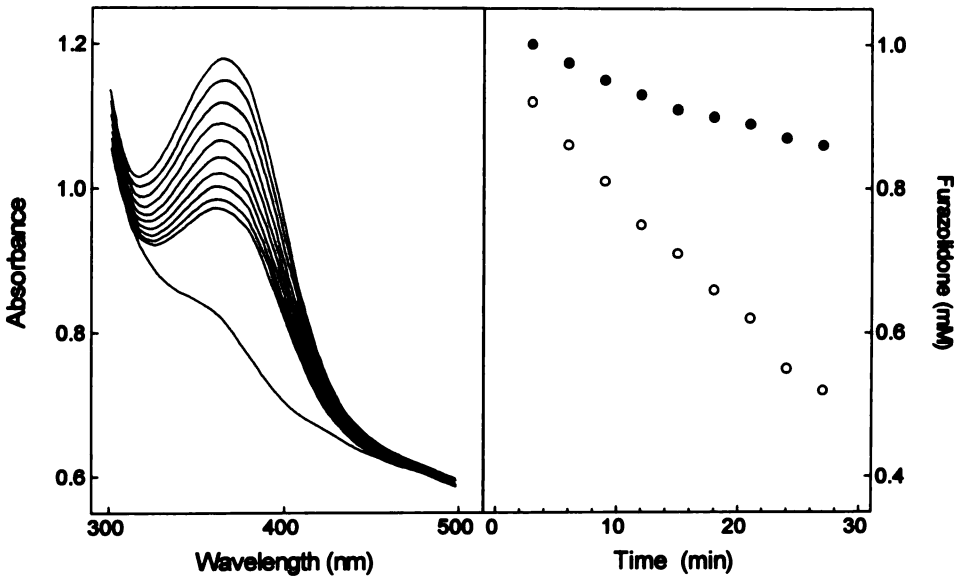

Fig. 6. Disappearance of the furazolidone absorption spectrum as a result of metabolism by undifferentiated Caco-2 cells. Samples of 100 μl cell suspensions containing 4 × 10^6 cells plus 1 mM furazolidone were prepared in flat glass capillaries, as described in Materials and Methods. No precipitation of cells occurred during the measurements due to the presence of 10% Ficoll in the buffer. a, Spectra recorded at 3-min intervals. *Bottom*, absorbance remaining after 2 hr. b, Time course of furazolidone reduction in the absence (○) or presence (●) of 400 μM DPI. Manipulation of the sample and alignment of the capillary in the spectrophotometer were not sufficiently fast to allow observation of an initial lag phase.

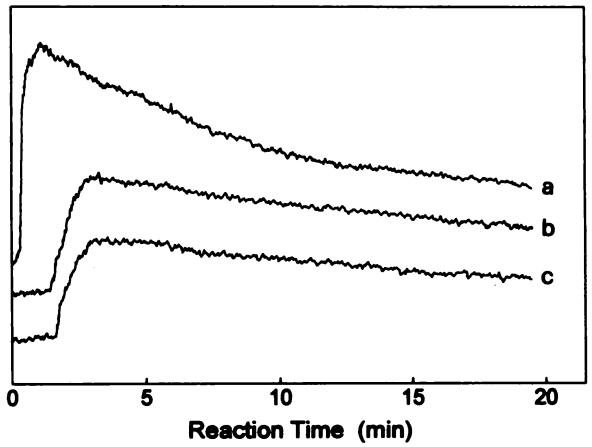

Fig. 7. Comparison between the kinetics of furazolidone radical formation seen with 2 × 10^6 differentiated Caco-2 cells (a), 1 × 10^6 differentiated cells (b), or 2 × 10^6 undifferentiated Caco-2 cells (c). All samples were incubated with 1 mM furazolidone.

TABLE 2

Oxygen consumption by Caco-2 cells exposed to furazolidone

Measurements were made in triplicate, as described in Materials and Methods. Basal respiration was blocked with 1 mM KCN before the addition of 560 μM furazolidone.

Cell type	Oxygen uptake
	nmol (min × 10^6 cells)$^{-1}$
Undifferentiated (7 days)	2.37 ± 0.17
+ KCN[a]	0
+ KCN[a] + furazolidone	1.19 ± 0.06
Differentiated (21 days)	3.45 ± 0.14
+ KCN[a]	0
+ KCN[a] + furazolidone	2.42 ± 0.11

[a] Cyanide concentration was 1 mM; identical results were obtained with 0.1 μM rotenone or 0.1 μM antimycin.

activity was seen on differentiation (Fig. 8). This result was in agreement with the above data from oxygen consumption and ESR measurements; however, expression of the reductase was clearly not affected by differentiation to the same extent as the typical differentiation marker enzymes sucrase-isomaltase and alkaline phosphatase or as the antioxidant enzyme catalase.

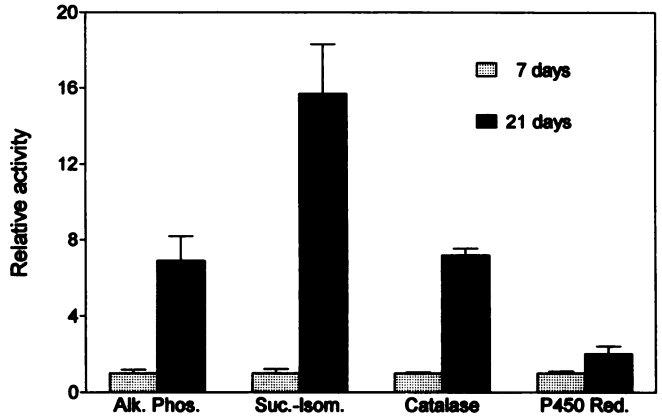

Fig. 8. Changes in enzyme activities of Caco-2 cells as a result of differentiation. The activities of alkaline phosphatase (*Alk. Phos.*), sucrase-isomaltase (*Suc.-Isom.*), catalase, and cytochrome P450 reductase (*P450 Red.*) were determined in undifferentiated cells (7-day culture) and differentiated cells (21-day culture). The increase on differentiation is shown relative to an activity of 1 for undifferentiated cells. The absolute enzyme activities expressed per 10^6 undifferentiated cells were as follows: sucrase-isomaltase, 1.36 ± 0.33 nmol min^{-1}; alkaline phosphatase, 69.1 ± 13.1 nmol min^{-1}; catalase, 15.0 ± 1.0 μmol min^{-1}; and cytochrome *c* (P450) reductase, 5.01 ± 0.61 nmol min^{-1}.

Differentiation of Caco-2 cells is known to lower their sensitivity to furazolidone (27), so the large increase in catalase activity observed in these cells suggested that cytotoxicity could be due to H_2O_2 formation. However, irreversible inactivation of the catalase by aminotriazole did not have an effect on the toxicity of furazolidone in differentiated cell cultures (Table 3), indicating that H_2O_2 production was not directly responsible for cell death. The same result was obtained after prolonged incubation (48 hr) with furazolidone (data not shown).

Discussion

The ESR method. The results of the current study demonstrate how noninvasive ESR measurements can be applied to investigate the metabolism of radical-generating drugs in intact cells. ESR spectroscopy has been used in a few previ-

TABLE 3

Effect of catalase inactivation on furazolidone toxicity to differentiated Caco-2 cells

Catalase activity was blocked by incubation with aminotriazole before the addition of furazolidone, as described in Materials and Methods. After 24-hr incubation with furazolidone, the cell viability (percent) was determined through the uptake of Neutral Red, measured by its absorption at 540 nm. Measurements were made in triplicate.

	No inhibitor		+ Aminotriazole	
	A_{540}	(%)	A_{540}	(%)
Control[a]	0.95 ± 0.04	(100)	0.88 ± 0.06	(100)
+ 220 μM Furazolidone	0.87 ± 0.05	(92)	0.80 ± 0.09	(91)
+ 440 μM Furazolidone	0.43 ± 0.09	(45)	0.38 ± 0.09	(43)

[a] Including the same concentration of dimethylsulfoxide as cells incubated with furazolidone.

ous reports on the cellular metabolism of nitrocompounds (35, 36) but not for systematic studies on the enzyme systems responsible for radical formation. There are particular problems involved in applying this technique to intact cells. The steady state concentration of furazolidone radicals is low, so high concentrations of cells are necessary to observe the signals. On the other hand, this elevated cell density may better reflect the actual conditions in the tissue. The radical can be detected at furazolidone concentrations of <50 μM, but the signal intensity and the rate of formation are low, making it difficult to precisely determine the kinetics. Therefore, saturating levels of furazolidone have been used to examine the effects of enzyme inhibitors. It is noteworthy that cell mortality during the experiments is quite low, considering that the cells are exposed to high concentrations of furazolidone and various inhibitors for a prolonged period under anaerobic conditions. Although furazolidone has been demonstrated to be noxious to Caco-2 cells (12, 27, 28), toxicity does not show up within the time of the ESR measurements.

The nitroanion free radical is an unstable intermediate, the level of which depends on the rates of generation and decay (Fig. 9). Formation takes place according to the following simple equation:

$$R\text{–}NO_2 + Enz^{red} \rightarrow R\text{–}NO_2^{\bullet -} + Enz^{ox} \quad (1)$$

In the absence of oxygen, the radical may either be reduced further or disappear through disproportionation; in both cases, the nitroso derivative is produced:

$$R\text{–}NO_2^{\bullet -} + Enz^{red} \rightarrow R\text{–}NO + Enz^{ox} + H_2O \quad (2)$$

$$2R\text{–}NO_2^{\bullet -} \rightarrow R\text{–}NO_2 + R\text{–}NO \quad (3)$$

Studies *in vitro* showed that radical decay can be ascribed essentially to Eq. 3 (9). However, Eq. 2 might be competitive at low radical levels because the rate of disproportionation is proportional to the square root of the radical concentration. The decrease in the radical steady state level is mainly due to consumption of the parent compound, as shown by the reappearance of the signal after the further addition of furazolidone. The results also demonstrate that the enzyme responsible for nitroreduction is not damaged during the process and that a sufficient supply of intracellular reducing equivalents is maintained throughout the experiments.

The site of furazolidone reduction. Although many different enzymes are able to reduce nitrofurans *in vitro*, the results reported in this study suggest that initial reduction

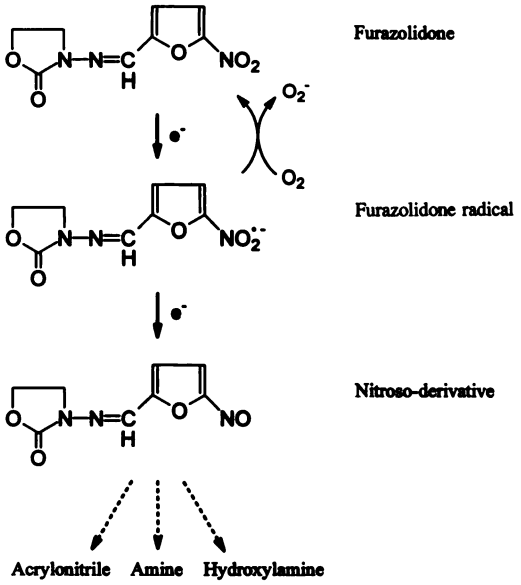

Fig. 9. Reductive metabolism of furazolidone.

by intact Caco-2 cells is almost exclusively due to cytochrome P450 reductase activity. Of all of the inhibitors tested, only the iodonium cations inhibit furazolidone radical formation. These compounds are efficient inhibitors of neutrophil and macrophage NADPH oxidases but have also been reported to inactivate other flavoproteins, including cytochrome P450 reductase from bovine and rat liver (37–39). Consistently, measurements of Caco-2 cytochrome *c* (P450) reductase activity carried out in the presence of DPI demonstrated complete inhibition of the enzyme (results not shown). For intact cells, DPI was found to be five times more potent than ID; this is in agreement with the pattern of inhibition previously reported for cytochrome P450 reductase (37–39). However, it should be kept in mind that the involvement of unknown reductases cannot be excluded.

It is possible that cytochrome P450 reductase is also directly involved in the formation of the two-electron reduced metabolite, the nitroso derivative. Direct reduction to the nitroso level does not take place with the isolated enzyme (40), but it is known that the catalytic properties of the enzyme are changed on purification. Isolated cytochrome P450 reductases are inhibited by concentrations of NADPH and nitrofuran substrates of >150 μM (41), and the rat liver enzyme is almost completely inactive in the presence of 1 mM nitrofurantoin (40). In contrast, the enzyme in intact rat liver microsomes is fully active at this nitrofurantoin concentration (40), which is in agreement with the results reported here for furazolidone. Clearly, the role of cytochrome P450 reductase activity *in vivo* cannot be deduced from the properties of the purified enzyme.

Despite the fact that cytochrome P450 enzymes are major activators of drugs, they do not appear to be involved in the initial steps of furazolidone activation in Caco-2 cells, as suggested by the failure of the inhibitors metyrapone, SKF-525A, and carbon monoxide to affect furazolidone radical formation. As these enzymes are known to mediate reduction of other redox active drugs, the results at first seem surprising, but they indirectly confirm recent observations by Goeptar *et al.* (42, 43), who found that single-electron reduction of

the quinone drugs adriamycin and mitomycin C by rat liver cytochrome P450 involves only the CYP2B1 isozyme. Although no direct evidence is available, it seems likely that furazolidone also will be reduced only by the CYP2B1 isoform, and it has been reported that this isozyme is not found in the Caco-2 cell line, which prevalently expresses the *CYP*1A family (26, 34).

DT-diaphorase is a two-electron donor, so reduction of furazolidone by this enzyme will not give rise to radical formation (14). If a significant fraction of the reduction were catalyzed in this way, inhibition by dicoumarol could be expected to shunt all furazolidone toward the cytochrome P450 reductase, resulting in increased radical formation. The lack of effect seen for dicoumarol thus indicates that DT-diaphorase does not have an important role in furazolidone reduction. This can also be concluded from the inhibitory effect of DPI shown in Fig. 6 because DT-diaphorase is not inhibited by DPI (39).

It should be emphasized that the findings reported in the current work refer only to the initial steps of furazolidone metabolism under anaerobic or strongly hypoxic conditions. It is possible that an enzyme like DT-diaphorase may be important during aerobic metabolism. Moreover, in intact cells the nitroso intermediate is reduced further to the hydroxylamine and other derivatives (10, 12), and different enzymes may be involved in these equations.

The effect of differentiation. The results demonstrate that furazolidone reduction by differentiated Caco-2 cells is only twice as efficient as for undifferentiated cells. The effect is probably due to the 2-fold higher cytochrome P450 reductase activity; thus, differentiation does not induce a second pathway of furazolidone metabolism. In comparison with the much larger increases in activity seen on differentiation for the characteristic enterocytic enzymes (22) as well as for other drug-metabolizing enzymes and for some antioxidant enzymes (26, 28), the change in cytochrome P450 reductase activity is rather modest, particularly when it is considered that half of the increase can be ascribed to the fact that differentiated cells have 50% more protein per cell than undifferentiated cells (data not shown). Therefore, this enzyme does not seem to be induced by differentiation. This could mean that expression of *CYP*1A1 on differentiation may produce a protein that is not enzymatically active, due to a shortage of cytochrome P450 reductase. In fact, the CYP1A1 activity of Caco-2 cells was reported to be only slightly dependent on the degree of differentiation (26).

Although production of radicals is increased in differentiated cells, they show decreased susceptibility to furazolidone in aerobiosis (27). The reason for this apparent contradiction is not known. Caco-2 cells have a very strong antioxidant defense, as documented by the activities of enzymes such as superoxide dismutase, glutathione peroxidase, and catalase (28, 29); this is important because one-electron reduction of furazolidone and similar drugs produces an increased intracellular flux of reactive oxygen species under aerobic conditions. Some antioxidative enzyme activities (notably, glutathione peroxidase and catalase) increase dramatically during the differentiation process (28, 29). However, the lack of effect of catalase inhibition on furazolidone-induced toxicity in differentiated cells indicates that the lower sensitivity of these cells cannot be ascribed to more efficient scavenging of H_2O_2. For furazolidone, as for the other nitroreductive drugs, the exact mechanism of cytotoxicity remains to be understood (1, 2).

In conclusion, the results of the current study demonstrate that noninvasive ESR spectroscopy used in combination with specific enzyme inhibitors allows the analysis of drug activation by intact cells. Among the various known nitroreductases, only cytochrome P450 reductase appears to be important for the initial activation of furazolidone in intact Caco-2 cells. Differentiation of Caco-2 cells does not change the pattern of activation, thus validating the use of undifferentiated cells for studies on reductive metabolism of furazolidone and similar drugs.

References

1. Adams, G. E., A. Breccia, E. M. Fielden, and P. Wardman, Eds. *Selective Activation of Drugs by Redox Processes*. Plenum Press, New York (1990).
2. Edwards, D. I. Nitroimidazole drugs: action and resistance mechanisms. I. Mechanisms of action. *J. Antimicrob. Chemother.* **31**:9–20 (1993)
3. McCalla, D. R. Mutagenicity of nitrofuran derivatives: review. *Environ. Mutagen.* **5**:745–765 (1983).
4. Wang C. Y., W. A. Croft, and G. T. Bryan. Tumor production in germ-free rats fed 5-nitrofurans. *Cancer Lett.* **21**:303–308 (1984).
5. Bremner, J. C. Assessing the bioreductive effectiveness of the nitroimidazole RSU1069 and its prodrug RB6145: with particular reference to *in vivo* methods of evaluation. *Cancer Metastasis Rev.* **12**:177–193 (1993).
6. Mason, R. P. Free radical metabolites of toxic chemicals and drugs as sources of oxidative stress, in *Biological Consequences of Oxidative Stress* (L. Spatz and A. D. Bloom, eds.). Oxford University Press, New York, 23–49 (1992).
7. Rossi, L., J. M. Silva, L. G. McGirr, and P. J. O'Brien. Nitrofurantoin-mediated oxidative stress cytotoxicity in isolated rat hepatocytes. *Biochem. Pharmacol.* **37**:3109–3117 (1988).
8. Adam, A., L. L. Smith, and G. M. Cohen. An assessment of the role of redox cycling in mediating the toxicity of paraquat and nitrofurantoin. *Environ. Health Perspect.* **85**:113–117 (1990).
9. Peterson, F. J., R. P. Mason, J. Hovsepian, and J. L. Holtzman. Oxygen-sensitive and -insensitive nitroreduction by *Escherichia coli* and rat hepatic microsomes. *J. Biol. Chem.* **254**:4009–4014 (1979).
10. Abraham, R. T., J. E. Knapp, M. B. Minnigh, L. K. Wong, M. A. Zemaitis and J. D. Alvin. Reductive metabolism of furazolidone by *Escherichia coli* and rat liver *in vitro*. *Drug Metab. Dispos.* **12**:732–741 (1984).
11. Vroomen, L. H. M., M. C. J. Berghmans, P. J. Van Bladeren, J. P. Groten, C. J. Wissink, and H. A. Kuiper. *In vivo* and *in vitro* metabolic studies of furazolidone: a risk evaluation. *Drug Metab. Rev.* **22**:663–676 (1990).
12. De Angelis, I., L. A. P. Hoogenboom, M. B. M. Huveneers-Oorsprong, F. Zucco, and A. Stammati. Established cell line for safety assessment of food contaminants: differing furazolidone toxicity to V79, HEp-2 and Caco-2 cells. *Food Chem. Toxicol.* **32**:481–488 (1994).
13. Raleigh, J. A., and C. J. Koch. Importance of thiols in the reductive binding of 2-nitroimidazoles to macromolecules. *Biochem. Pharmacol.* **40**:2457–2464 (1990).
14. Rauth, A. M., R. S. Marshall, and B. L. Kuehl. Cellular approaches to bioreductive drug mechanisms. *Cancer Metastasis Rev.* **12**:153–164 (1993).
15. Hajjar, R. J., R. Liao, J. B. Young, F. Fuleihan, M. G. Glass, and J. K. Gwathmey. Pathophysiological and biochemical characterization of an avian model of dilated cardiomyopathy: comparison to findings in human dilated cardiomyopathy. *Cardiovasc. Res.* **27**:2212–2221 (1993).
16. Pettinger, W. A., F. G. Soyangco, and J. A. Oates. Inhibition of monoamine oxidase in man by furazolidone. *Clin. Pharmacol. Ther.* **2**:442–447 (1968).
17. Ali, B. H. Pharmacology and toxicity of furazolidone in man and animals: some recent research. *Gen. Pharmacol.* **20**:557–563 (1989).
18. Pinto, M., S. Robine-Leon, M.-D. Appay, M. Kedinger, N. Triadou, E. Dussaulx, B. Lacroix, P. Simon-Assmann, K. Haffen, J. Fogh, and A. Zweibaum. Enterocyte-like differentiation and polarization of the human colon carcinoma cell line Caco-2 in culture. *Biol. Cell* **47**:323–330 (1983).
19. Grasset, E., M. Pinto, E. Dussaulx, A. Zweibaum, and J. F. Desjeux. Epithelial properties of human colonic carcinoma cell line Caco-2: electrical parameters. *Am. J. Physiol.* **247**:C260–C267 (1984).
20. Grasset, E., J. Bernareu, and M. Pinto. Epithelial properties of human colonic carcinoma cell line Caco-2: effect of segretagogues. *Am. J. Physiol.* **248**:C410–C418 (1985).
21. Hidalgo, I. J., J. T. Raub, and R. T. Borchardt. Characterization of the human colon carcinoma cell line (Caco-2) as a model system for intestinal epithelial permeability. *Gastroenterology* **96**:736–749 (1989).
22. Matsumoto, H., R. H. Erickson, J. R. Gum, M. Yoshioka, E. Gum, and Y. S. Kim. Biosynthesis of alkaline phosphatase during differentiation of the human colon cancer cell line Caco-2. *Gastroenterology* **98**:1199–1207 (1990).

23. Peters, W. H. N., and H. M. J. Roelofs. Time-dependent activity and expression of glutathione S-transferases in the human colon adenocarcinoma cell line Caco-2. *Biochem. J.* **264:**613–616 (1989).
24. Oude Elferink, R. P. J., C. T. M. Bakker, and P. L. M. Jansen. Glutathione-conjugate transport by human colon adenocarcinoma cells (Caco-2 cells). *Biochem. J.* **290:**759–764 (1993).
25. Baker, S. S., and R. D. Baker, Jr. Caco-2 cell metabolism of oxygen-derived radicals. *Dig. Dis. Sci.* **38:**2273–2280 (1993).
26. Boulenc, X., M. Bourrie, I. Fabre, C. Roque, H. Joyeux, Y. Berger, and G. Fabre. Regulation of cytochrome P450IA1 gene expression in a human intestinal cell line, Caco-2. *J. Pharmacol. Exp. Ther.* **263:**1471–1478 (1992).
27. Vincentini, O., I. De Angelis, A. Stammati, and F. Zucco. Functional alterations induced by the food contaminant furazolidone on the human tumoral intestinal cell line Caco-2. *Toxicol. In Vitro* **7:**403–406 (1993).
28. Zucco, F., I. De Angelis, O. Vincentini, L. Rossi, C. Steinkühler, and A. Stammati. Potentiality of the human intestinal cell line Caco-2 in toxicological investigation. *In Vitro Toxicol.* **7:**107–112 (1994).
29. Baker, S. S., and R. D. Baker, Jr. Antioxidant enzymes in the differentiated Caco-2 cell line. *In Vitro Cell. & Dev. Biol. Anim.* **28:**643–647 (1992).
30. Dallner, G. Isolation of rough and smooth microsomes. *Methods Enzymol.* **31:**191–201 (1974).
31. Borenfreund, E., and J. A. Puerner. Toxicity determined *in vitro* by morphological alterations and neutral red absorption. *Toxicol. Lett.* **24:**119–124 (1985).
32. Strobel, H. W., and J. D. Dignam. Purification and properties of NADPH cytochrome P450 reductase. *Methods Enzymol.* **52:**89–96 (1978).
33. Hodnick, W. F., and A. C. Sartorelli. Reductive activation of mitomycin C by NADH-cytochrome b_5 reductase. *Proc. Am. Assoc. Cancer Res.* **32:**397 (1991).
34. Rosenberg, D. W., and T. Leff. Regulation of cytochrome P450 in cultured human colonic cells. *Arch. Biochem. Biophys.* **300:**186–192 (1993).
35. Lloyd, D., and J. Z. Pedersen. Metronidazole radical anion generation *in vivo* in *Trichomonas vaginalis*: oxygen quenching is enhanced in a drug-resistant strain. *J. Gen. Microbiol.* **131:**87–92 (1985).
36. Rao, D. N. R., S. Jordan, and R. P. Mason. Generation of nitro radical anions of some 5-nitrofurans, and 2- and 5-nitroimidazoles by rat hepatocytes. *Biochem. Pharmacol.* **37:**2907–2913 (1988).
37. Doussier, J., and P. V. Vignais. Diphenylene iodonium as an inhibitor of the NADPH oxidase complex of bovine neutrophils. *Eur. J. Biochem.* **208:**61–71 (1992).
38. Tew, D. G. Inhibition of cytochrome P450 reductase by the diphenyliodonium cation: kinetic analysis and covalent modifications. *Biochemistry* **32:**10209–10215 (1993).
39. Silva, J. M., and P. J. O'Brien. Molecular mechanisms of SR 4233-induced hepatocyte toxicity under aerobic versus hypoxic conditions. *Br. J. Cancer* **68:**484–491 (1993).
40. Holtzman, J. L., D. L. Crankshaw, F. J. Peterson, and C. F. Polnaszek. The kinetics of the aerobic reduction of nitrofurantoin by NADPH-cytochrome P-450 (*c*) reductase. *Mol. Pharmacol.* **20:**669–673 (1981).
41. Iscan, M. Comparative studies of sheep lung and liver nitrofurantoin reductase. *Comp. Biochem. Physiol. C Comp. Pharmacol.* **106:**579–584 (1993).
42. Goeptar, A. R., J. M. te Koppele, E. K. Lamme, J. M. Piqué, and N. P. E. Vermeulen. Cytochrome P450 2B1-mediated one-electron reduction of adriamycin: a study with rat liver microsomes and purified enzymes. *Mol. Pharmacol.* **44:**1267–1277 (1993).
43. Goeptar, A. R., E. J. Groot, H. Scheerens, J. N. N. Commandeur, and N. P. E. Vermeulen. Cytotoxicity of mitomycin C and adriamycin in freshly isolated rat hepatocytes: the role of cytochrome P450. *Cancer Res.* **54:**2411–2418 (1994).
44. Nebert, D. W., D. R. Nelson, M. J. Coon, R. W. Estabrook, R. Feyeresein, Y. Fujii-Kuriyama, F. J. Gonzalez, F. P. Guengerich, I. C. Gunsalus, E. F. Johnson, T. L. Loper, R. Soto, M. R. Waterman, and D. J. Waxman. The P450 superfamily: update on new sequences, gene mapping, and recommended nomenclature. *DNA Cell Biol.* **10:**1–14 (1991)

Send reprint requests to: Dr. Luisa Rossi, Department of Biology, University of Rome "Tor Vergata," via della Ricerca Scientifica, Rome 00133, Italy. E-mail:Biologia@vaxtov.roma2.infn.it